

Gluino two-body decays at full one-loop level in the MSSM with quark-flavour violation

Helmut Eberl*, **Elena Ginina**,

Institut für Hochenergiephysik der Österreichischen Akademie der Wissenschaften

E-mail: helmut.eberl@oeaw.ac.at, elena.ginina@oeaw.ac.at

Keisho Hidaka

Department of Physics, Tokyo Gakugei University, Koganei, Tokyo 184-8501, Japan

E-mail: hidaka@u-gakugei.ac.jp

We study the two-body decays of the gluino at full one-loop level in the Minimal Supersymmetric Standard Model with quark-flavour violation (QFV) in the squark sector. The renormalization is done in the $\overline{\text{DR}}$ scheme and hard gluon and photon radiations are included by adding the corresponding three-body decay widths. In the numerics the dependence of the gluino decay widths on the QFV parameters is discussed with special emphasis put on the separation of the electroweak and the SUSY QCD corrections. The main dependence stems from the $\tilde{c}_R - \tilde{t}_R$ mixing in the decays to up-type squarks because there hold strong constraints from B-physics on the other quark-flavour mixing parameters. Including the full one-loop corrections, the changes of the gluino decay widths are mostly negative and of the order of about -10%. The QFV part stays small in the total width but can vary up to -8% for the decay width into the lightest squark. For the corresponding branching ratio, however, the effect is smaller by at least a factor of two. The electroweak corrections can become 35% of the SUSY QCD corrections.

13th International Symposium on Radiative Corrections (Applications of Quantum Field Theory to Phenomenology)

25-29 September, 2017

St. Gilgen, Austria

*Speaker.

1. Introduction

Although there is no sign of new particles yet, the MSSM is still favoured as a discoverable theory beyond the SM and will be searched for with high priority at all experiments. SUSY particle decay chains have been extensively studied during the last two decades. Especially relevant are the decays of strongly interacting squarks and gluinos because they can be produced at LHC copiously. There exist an enormous number of MSSM studies. Nevertheless it has yet unstudied potential related to more general treatment of its squark sector parameters. Despite the stringent constraints from B and K physics, such parameters can lead to quark-flavour violation (QFV) and can change the phenomenological observables significantly.

In [1] the two-body decays of the gluino in the MSSM in the quark flavour conserving (QFC) case were studied including the one-loop SUSY-QCD corrections, and the full one-loop corrections allowing complex parameters were presented in [2]. Studies of these decays including general quark-flavour violation in the squark sector at tree-level are in [3, 4]. In [5] three-body decays of the gluino at tree-level are discussed.

In this work based on [6] we study the two-body decays of the gluino at full one-loop level in the MSSM with quark-flavour violation in the squark sector. For further details see also the PhD thesis of Sebastian Frank [7]. The renormalization is done in the $\overline{\text{DR}}$ scheme and hard gluon and photon radiations are included by adding the corresponding three-body decay widths.

2. QFV parameters

In the SM QFV is within the Cabibbo-Kobayashi-Maskawa (CKM) matrix. In the general MSSM there are two concepts:

1. *Minimal quark flavour violation* - no new sources of QFV, in the super-CKM basis the squarks undergo the same rotations like the quarks, all flavour violating entries are related to the CKM matrix,
2. *Non-minimal quark flavour violation* - new sources of QFV, independent of the CKM, considered as free parameters in the theory.

In this study 2. is assumed.

The hermitian 6×6 squark mass matrix in the super-CKM basis is

$$\mathcal{M}_{\tilde{q}}^2 = \begin{pmatrix} \mathcal{M}_{\tilde{q},LL}^2 & \mathcal{M}_{\tilde{q},LR}^2 \\ \mathcal{M}_{\tilde{q},RL}^2 & \mathcal{M}_{\tilde{q},RR}^2 \end{pmatrix}, \quad (2.1)$$

with $\tilde{q} = \tilde{u}, \tilde{d}$. The 3×3 blocks in eq. (2.1) for the up squarks are

$$\begin{aligned} \mathcal{M}_{\tilde{u},LL}^2 &= V_{\text{CKM}} M_Q^2 V_{\text{CKM}}^\dagger + D_{\tilde{u},LL} \mathbf{1} + \hat{m}_u^2, \\ \mathcal{M}_{\tilde{u},RR}^2 &= M_U^2 + D_{\tilde{u},RR} \mathbf{1} + \hat{m}_u^2, \\ \mathcal{M}_{\tilde{u},RL}^2 &= \mathcal{M}_{\tilde{u},LR}^{2\dagger} = \frac{v_2}{\sqrt{2}} T_U - \mu^* \hat{m}_u \cot \beta. \end{aligned} \quad (2.2)$$

$v_2 = \sqrt{2} \langle H_2^0 \rangle$, $M_{Q,U}^2$ are hermitian soft SUSY-breaking squark mass matrices and T_U is a soft SUSY-breaking trilinear coupling matrix. The ratio of the vacuum expectation values of the neutral Higgs fields $v_2/v_1 = \tan\beta$, μ is the higgsino mass parameter, and $\hat{m}_{u,d}$ are the diagonal mass matrices of the up- and down-type quarks. Furthermore, $D_{\bar{q},LL} = \cos 2\beta m_Z^2 (T_3^q - e_q \sin^2 \theta_W)$ and $D_{\bar{q},RR} = e_q \sin^2 \theta_W \cos 2\beta m_Z^2$, where T_3^q and e_q are the isospin and electric charge of the quarks (squarks), respectively, and θ_W is the weak mixing angle. We approximate the V_{CKM} by the unit matrix. Analogous formulas hold for the down squarks.

The eigenvalue problems for up and down squarks can be written as

$$\begin{aligned}
 U^{\bar{u}} \mathcal{M}_{\bar{u}}^2 (U^{\bar{u}})^\dagger &= \text{diag}(m_{\bar{u}_1}^2, \dots, m_{\bar{u}_6}^2), \\
 U^{\bar{d}} \mathcal{M}_{\bar{d}}^2 (U^{\bar{d}})^\dagger &= \text{diag}(m_{\bar{d}_1}^2, \dots, m_{\bar{d}_6}^2),
 \end{aligned}
 \quad \text{with} \quad
 \begin{pmatrix} \tilde{u}_1 \\ \tilde{u}_2 \\ \tilde{u}_3 \\ \tilde{u}_4 \\ \tilde{u}_5 \\ \tilde{u}_6 \end{pmatrix} = U^{\bar{u}} \cdot \begin{pmatrix} \tilde{u}_L \\ \tilde{c}_L \\ \tilde{t}_L \\ \tilde{u}_R \\ \tilde{c}_R \\ \tilde{t}_R \end{pmatrix}, \quad
 \begin{pmatrix} \tilde{d}_1 \\ \tilde{d}_2 \\ \tilde{d}_3 \\ \tilde{d}_4 \\ \tilde{d}_5 \\ \tilde{d}_6 \end{pmatrix} = U^{\bar{d}} \cdot \begin{pmatrix} \tilde{d}_L \\ \tilde{s}_L \\ \tilde{b}_L \\ \tilde{d}_R \\ \tilde{s}_R \\ \tilde{b}_R \end{pmatrix}. \quad (2.3)$$

QFV is expressed by dimensionless parameters, in the up-type squark sector they are

$$\delta_{\alpha\beta}^{LL} \equiv M_{Q\alpha\beta}^2 / \sqrt{M_{Q\alpha\alpha}^2 M_{Q\beta\beta}^2}, \quad (2.4)$$

$$\delta_{\alpha\beta}^{uRR} \equiv M_{U\alpha\beta}^2 / \sqrt{M_{U\alpha\alpha}^2 M_{U\beta\beta}^2}, \quad (2.5)$$

$$\delta_{\alpha\beta}^{uRL} \equiv (v_2/\sqrt{2}) T_{U\alpha\beta} / \sqrt{M_{U\alpha\alpha}^2 M_{Q\beta\beta}^2}, \quad (2.6)$$

with $\alpha, \beta = 1, 2, 3$ ($\alpha \neq \beta$) denoting the quark flavours u, c, t . Analogous formulas hold for the sdown parameters $\delta_{\alpha\beta}^{dRR}$ and $\delta_{\alpha\beta}^{dRL}$.

3. Gluino two-body decay widths

The explicit form of the tree-level width is

$$\begin{aligned}
 \Gamma^0(\tilde{g} \rightarrow \tilde{q}_i^* q_g) &= \frac{\lambda^{1/2}(m_{\tilde{g}}^2, m_{\tilde{q}_i}^2, m_{q_g}^2)}{32 m_{\tilde{g}}^3} \alpha_s \left(\left(|U_{i,g}^{\tilde{q}}|^2 + |U_{i,g+3}^{\tilde{q}}|^2 \right) (m_{\tilde{g}}^2 - m_{\tilde{q}_i}^2 + m_{q_g}^2) \right. \\
 &\quad \left. - 4 m_{\tilde{g}} m_{q_g} \text{Re} \left(U_{i,g}^{\tilde{q}*} U_{i,g+3}^{\tilde{q}} \right) \right)
 \end{aligned} \quad (3.1)$$

with $i = 1, \dots, 6$ (no summation), $q = u, d$, and the subscript g is the quark-generation index.

In order to obtain an ultraviolet (UV) convergent result at one-loop level we employ the SUSY invariant dimensional reduction ($\overline{\text{DR}}$) regularisation scheme, which implies that all tree-level input parameters of the Lagrangian are defined at the scale $Q = M_3 \approx m_{\tilde{g}}$. Since in this scheme the tree-level couplings $g_{L,R}^i$ are defined at the scale Q , they do not receive further finite shifts due to radiative corrections. The physical scale independent masses and fields are obtained from the $\overline{\text{DR}}$ ones using on-shell renormalisation conditions.

The renormalised one-loop partial decay widths are given by

$$\begin{aligned} \Gamma(\tilde{g} \rightarrow \tilde{q}_i^* q_g) &= \Gamma^0(\tilde{g} \rightarrow \tilde{q}_i^* q_g) + \Delta\Gamma(\tilde{g} \rightarrow \tilde{q}_i^* q_g), \quad \text{with} \\ \Delta\Gamma(\tilde{g} \rightarrow \tilde{q}_i^* q_g) &= \frac{\lambda^{1/2}(m_{\tilde{g}}^2, m_{\tilde{q}_i}^2, m_{q_g}^2)}{512 \pi m_{\tilde{g}}^3} \text{Re}(\mathcal{M}_0^\dagger \mathcal{M}_1), \quad \text{and} \\ \text{Re}(\mathcal{M}_0^\dagger \mathcal{M}_1) &= \text{Re} \left((g_L^{i*} \Delta g_L + g_R^{i*} \Delta g_R)(m_{\tilde{g}}^2 - m_{\tilde{q}_i}^2 + m_{q_g}^2) + 2m_{\tilde{g}} m_{q_g} (g_L^{i*} \Delta g_R + g_R^{i*} \Delta g_L) \right), \end{aligned} \quad (3.2)$$

where \mathcal{M}_0 is the tree-level, and \mathcal{M}_1 the one-loop amplitude. The Q independent renormalised shifts to the left and right couplings can be split,

$$\Delta g_{L,R} = \delta g_{L,R}^v + \delta g_{L,R}^w + \delta g_{L,R}^c, \quad (3.3)$$

with v stands for the vertex corrections, w for the corrections of the wave functions, and c for the coupling counter terms. Further details including also the treatment of the infrared divergences can be found in [6] and in [7]. The full one-loop two-body decay width eq. (3.2) includes one-loop shifts from SQCD (gluon and gluino) and EW (electroweak including also the photon) corrections,

$$\Gamma(\tilde{g} \rightarrow \tilde{q}_i^* q_g) = \Gamma^0(\tilde{g} \rightarrow \tilde{q}_i^* q_g) + \Delta\Gamma^{\text{SQCD}}(\tilde{g} \rightarrow \tilde{q}_i^* q_g) + \Delta\Gamma^{\text{EW}}(\tilde{g} \rightarrow \tilde{q}_i^* q_g). \quad (3.4)$$

For illustration, all one-loop vertex graphs are shown in Fig 1. The first line gives contributions to SQCD and the other ones to EW.

In the numerical study the notation $\Gamma(\tilde{g} \rightarrow \tilde{q}_i q_g) = \Gamma(\tilde{g} \rightarrow \tilde{q}_i^* q_g) + \Gamma(\tilde{g} \rightarrow \tilde{q}_i \bar{q}_g)$ is used. This is equivalent with $2\Gamma(\tilde{g} \rightarrow \tilde{q}_i^* q_g)$ when CP is conserved, which is the case in this study.

4. Numerical results

The gluino two-body widths and branching ratios are calculated with the publicly available numerical code FVSFOLD, developed by Sebastian Frank [7]. For building FVSFOLD also the packages FeynArts [8, 9] and FormCalc [10] were used. FVSFOLD needs LoopTools [10] based on FF [11]. The counter terms are included by ourselves. The code used here is cross-checked by SARAH (personal correspondence with F. Staub). For calculating the h^0 mass and the low-energy observables, especially those ones in the B-sector we use SPheno v3.3.3 [12, 13]. The experimental and theoretical constraints taken into account are presented in Appendix B of [6].

First we fix a reference scenario which fulfills all constraints, see Table 1. Then we vary the QFV parameters within the allowed region. The MSSM mass spectrum is presented in Table 2. We see that our reference point violates QF explicitly and we have approximately gauge unification. Table 3 shows the flavour decompositions of the $\tilde{u}_{1,2}$ and $\tilde{d}_{1,2}$ squarks. The \tilde{u}_1 squark is a strong mixture of \tilde{c}_R and \tilde{t}_R , with a tiny contribution from \tilde{c}_L , and the \tilde{u}_2 squark is mainly \tilde{t}_L , with a tiny contribution from \tilde{c}_R . The \tilde{d}_1 is a mixture of \tilde{s}_R and \tilde{b}_R , and \tilde{d}_2 is a pure \tilde{b}_L . The decays of \tilde{g} into the lightest two sups and sdowns are possible with the branching ratios $B(\tilde{g} \rightarrow \tilde{u}_1 c) \approx 17\%$, $B(\tilde{g} \rightarrow \tilde{d}_1 s) \approx 18\%$, $B(\tilde{g} \rightarrow \tilde{u}_1 t) = B(\tilde{g} \rightarrow \tilde{d}_1 b) \approx 27\%$, $B(\tilde{g} \rightarrow \tilde{u}_2 t) \approx 5\%$. The total two-body width including the full one-loop contribution, $\Gamma(\tilde{g} \rightarrow \tilde{q}q) = 70 \text{ GeV}$. The tree-level width $\Gamma^0(\tilde{g} \rightarrow \tilde{q}q) = 75 \text{ GeV}$.

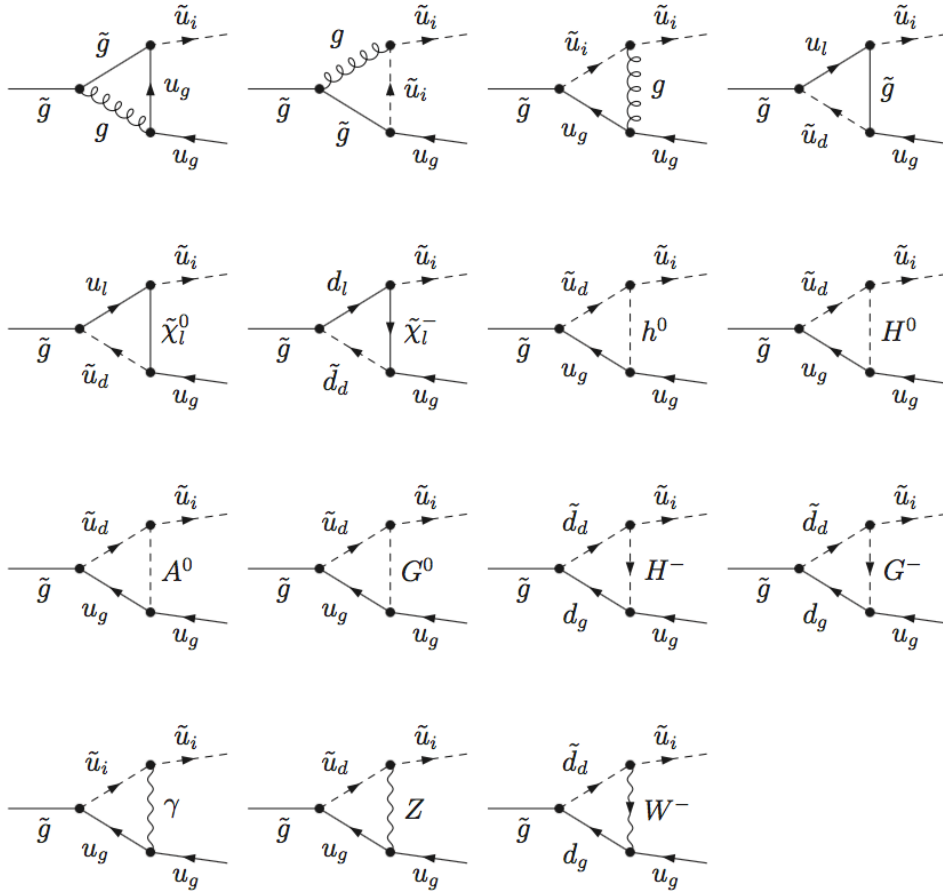


Figure 1: Feynman graphs of all one-loop vertex contributions to $\Gamma(\tilde{g} \rightarrow \tilde{q}_i^* q_g)$, $i = 1, \dots, 6$, $g = 1, 2, 3$.

The QFV parameters δ_{23}^{uLR} , δ_{23}^{uRL} , δ_{23}^{dLR} , and δ_{23}^{dRL} are constrained from the vacuum stability conditions. Thus they must remain rather small. A large δ_{23}^{LL} is not possible because it violates B-physics constraints such as that for $B_s \rightarrow \mu^+ \mu^-$. However, large right-right mixing in both \tilde{u} and \tilde{d} sectors is allowed. Therefore, in the following we only need to show diagrams with dependences on δ_{23}^{uRR} and δ_{23}^{dRR} .

Table 1: QFV reference scenario: all parameters are calculated at $Q = M_3 = 3 \text{ TeV} \simeq m_{\tilde{g}}$, except for m_{A^0} which is the pole mass of A^0 , and $T_{U33} = 2500 \text{ GeV}$ (corresponding to $\delta_{33}^{uRL} = 0.06$). All other squark parameters are zero.

M_1	M_2	M_3	μ	$\tan \beta$	m_{A^0}
500 GeV	1000 GeV	3000 GeV	500 GeV	15	3000 GeV

	$\alpha = 1$	$\alpha = 2$	$\alpha = 3$
$M_{Q\alpha\alpha}^2$	3200^2 GeV^2	3000^2 GeV^2	2600^2 GeV^2
$M_{U\alpha\alpha}^2$	3200^2 GeV^2	3000^2 GeV^2	2600^2 GeV^2
$M_{D\alpha\alpha}^2$	3200^2 GeV^2	3000^2 GeV^2	2600^2 GeV^2

δ_{23}^{LL}	δ_{23}^{uRR}	δ_{23}^{uRL}	δ_{23}^{uLR}	δ_{23}^{dRR}	δ_{23}^{dRL}	δ_{23}^{dLR}
0.01	0.7	0.04	0.07	0.7	0	0

Table 2: Physical masses of the particles in GeV for the scenario of Table 1.

$m_{\tilde{\chi}_1^0}$	$m_{\tilde{\chi}_2^0}$	$m_{\tilde{\chi}_3^0}$	$m_{\tilde{\chi}_4^0}$	$m_{\tilde{\chi}_1^+}$	$m_{\tilde{\chi}_2^+}$
460	500	526	1049	493	1049

m_{h^0}	m_{H^0}	m_{A^0}	m_{H^+}
125	3000	3000	3001

$m_{\tilde{g}}$	$m_{\tilde{u}_1}$	$m_{\tilde{u}_2}$	$m_{\tilde{u}_3}$	$m_{\tilde{u}_4}$	$m_{\tilde{u}_5}$	$m_{\tilde{u}_6}$
3154	1602	2686	3087	3295	3300	3692

$m_{\tilde{d}_1}$	$m_{\tilde{d}_2}$	$m_{\tilde{d}_3}$	$m_{\tilde{d}_4}$	$m_{\tilde{d}_5}$	$m_{\tilde{d}_6}$
1662	2689	3087	3295	3301	3747

Table 3: Flavour decomposition of $\tilde{u}_{1,2}$ and $\tilde{d}_{1,2}$ for the scenario of Table 1. Shown are the squared coefficients.

	\tilde{u}_L	\tilde{c}_L	\tilde{t}_L	\tilde{u}_R	\tilde{c}_R	\tilde{t}_R
\tilde{u}_1	0	0.004	0	0	0.38	0.61
\tilde{u}_2	0	0.001	0.99	0	0.006	0

	\tilde{d}_L	\tilde{s}_L	\tilde{b}_L	\tilde{d}_R	\tilde{s}_R	\tilde{b}_R
\tilde{d}_1	0	0	0	0	0.4	0.6
\tilde{d}_2	0	0	1	0	0	0

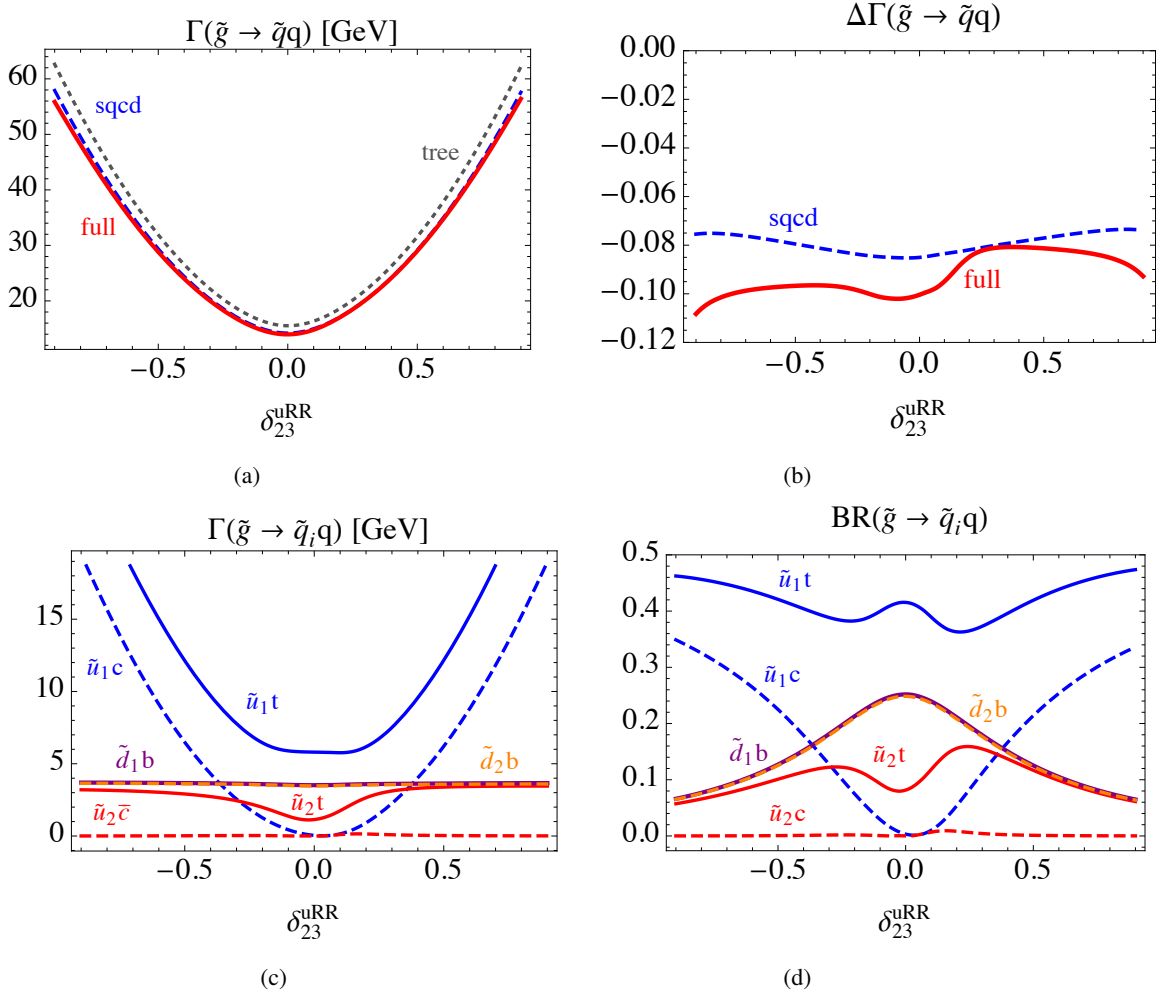


Figure 2: (a) Total two-body decay width $\Gamma(\tilde{g} \rightarrow \tilde{q}q)$ at tree-level, SQCD one-loop and full one-loop corrected as functions of the QFV parameter δ_{23}^{uRR} ; (b) $\Delta\Gamma(\tilde{g} \rightarrow \tilde{q}q)$ being the SQCD one-loop and the full one-loop corrections to $\Gamma(\tilde{g} \rightarrow \tilde{q}q)$ relative to the tree-level width; (c) Partial decay widths and (d) branching ratios of the kinematically allowed individual two-body channels at full one-loop level as functions of δ_{23}^{uRR} . All the other parameters are fixed as in Table 1, except $\delta_{23}^{uRL} = \delta_{23}^{uLR} = 0.03$.

We first discuss the dependences on the QFV parameter δ_{23}^{uRR} . Fig. 2(a) shows a strong dependence of $\Gamma(\tilde{g} \rightarrow \tilde{q}q)$ which stems mainly from the kinematic prefactor, see Section 3. The SQCD correction shown in Fig. 2(b) is only weakly dependent on δ_{23}^{uRR} and is about -8%. The EW correction can become -3% for large and negative values of δ_{23}^{uRR} . In Fig. 2(c) the partial widths of the $\tilde{d}_{1,2}b$ modes coincide because $m_{\tilde{d}_1} \approx m_{\tilde{d}_2}$. The same holds for the branching ratios in Fig. 2(d). For $\delta_{23}^{uRR} \approx 0$ the width of $\tilde{g} \rightarrow \tilde{u}_1 c$ becomes tiny because then \tilde{u}_1 is mainly \tilde{t}_R as all the other QFV δ 's are relatively small.

The relative contributions of the one-loop SQCD and the full one-loop part in terms of the tree-level result for the decay $\tilde{g} \rightarrow \tilde{u}_1 t$ as a function of δ_{23}^{uRR} are shown in Fig. 3(a) for the partial decay width and in Fig. 3(b) for the branching ratio. The SQCD corrections vary in the range of -8% to -10%. The EW correction is much stronger dependent on δ_{23}^{uRR} , varying between 1% down to -8%. The effects are similar in the branching ratio (b), but weaker. Out of the squark masses

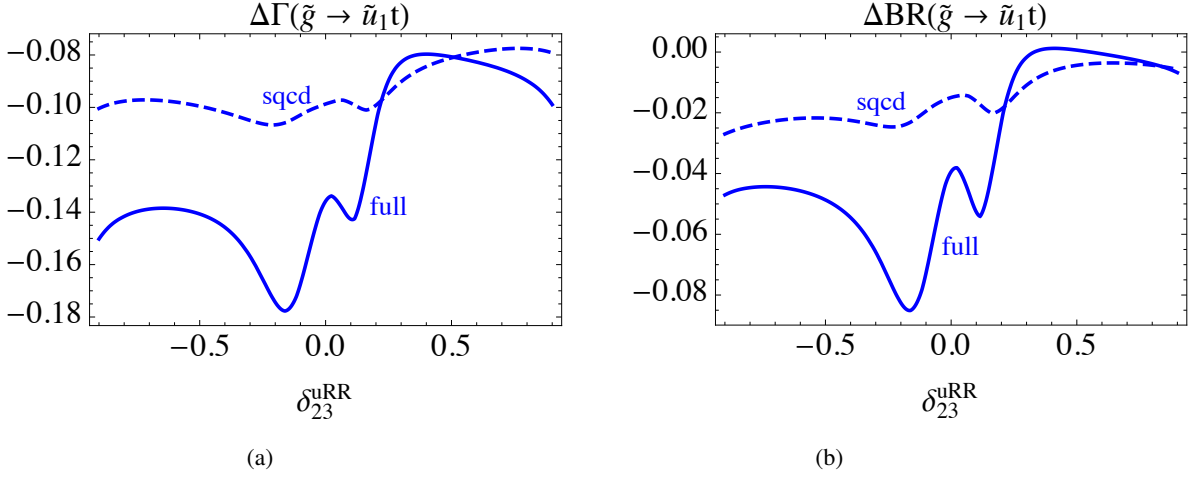


Figure 3: $\Delta\Gamma$ and ΔBR denote the SQCD one-loop and the full one-loop corrections relative to the tree-level result for the decay $\tilde{g} \rightarrow \tilde{u}_1 t$ as a function of δ_{23}^{uRR} ; (a) and (b) is for the partial width and the branching ratio, respectively. The other parameters are fixed as in Fig. 2.

only $m_{\tilde{u}_1}$ is strongly dependent on δ_{23}^{uRR} . The wiggles stem from the complex structures of the QFV one-loop contributions because no additional channel opens but those visible in Figs. 2(c) and 2(d).

Similar to Figs. 2 and 3 we have studied the dependence on the sdown right-right parameter δ_{23}^{dRR} . The dependence of the total gluino width is similar to that of δ_{23}^{uRR} but the EW contribution is smaller, up to 2%. The individual partial widths show a similar picture with $\tilde{u} \leftrightarrow \tilde{d}$ compared to the ones given in Figs. 2(c) and 2(d). The corrections to the channels $\tilde{g} \rightarrow \tilde{d}_1 b$ are smaller than for $\tilde{g} \rightarrow \tilde{u}_1 t$. It is interesting that for $\tilde{g} \rightarrow \tilde{u}_1 t$ the width varies by about -3% in the allowed range of δ_{23}^{dRR} . This effect stems from the \tilde{d} loops in gluino wave-function correction.

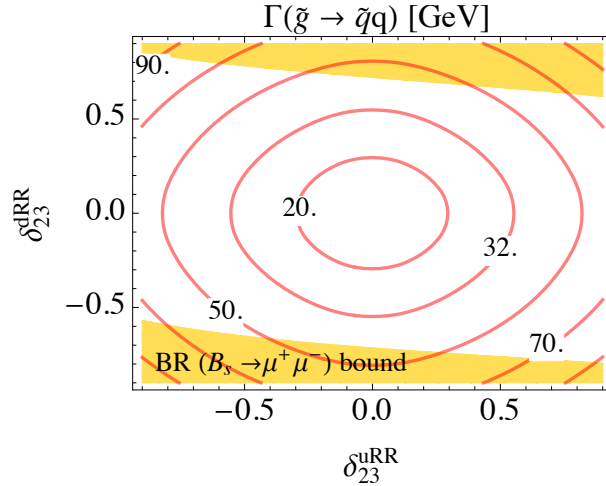


Figure 4: Total two-body decay width $\Gamma(\tilde{g} \rightarrow \tilde{q} q)$ at full one-loop level as a function of the QFV parameters δ_{23}^{dRR} and δ_{23}^{uRR} . All the other parameters are given in Table 1, except $\delta_{23}^{uRL} = \delta_{23}^{uLR} = 0.01$.

Fig. 4 shows the dependence of the total gluino width at one-loop level on the right-right mixing parameter of both the \tilde{u} and \tilde{d} sectors. The width varies from 20 GeV up to 90 GeV in the

allowed region.

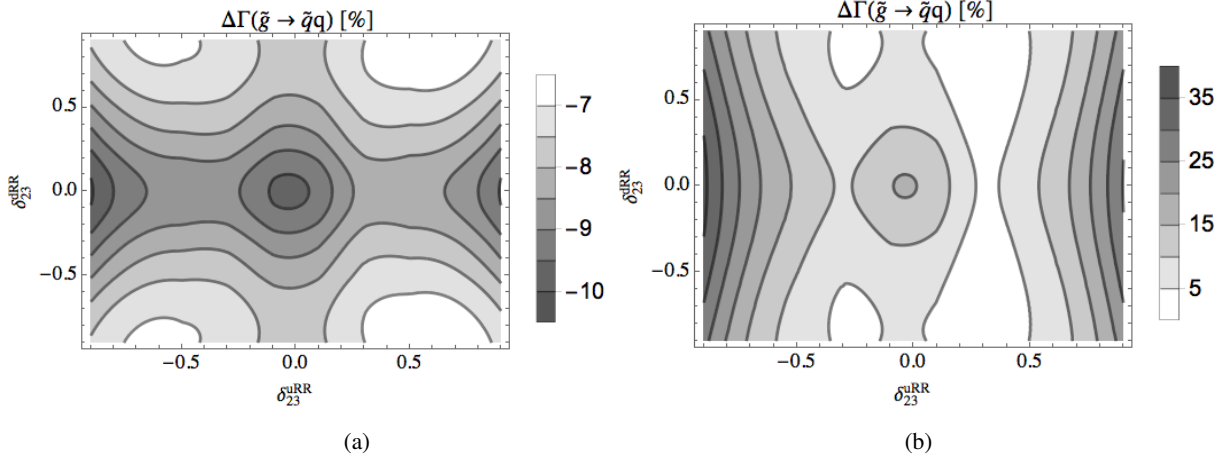


Figure 5: $\Delta\Gamma$ denotes in (a) the full one-loop contribution in terms of the total tree-level width, in (b) the EW contribution relative to the SQCD contribution. Both plots are given as a function of the QFV parameters δ_{23}^{uRR} and δ_{23}^{dRR} . All the other parameters are given in Table 1, except $\delta_{23}^{uRL} = \delta_{23}^{uLR} = 0.01$.

In Fig. 5(a) the full one-loop part in terms of the tree-level result and in Fig. 5(b) the EW contribution relative to the SQCD contribution are shown for the total two-body gluino decay width as a function of δ_{23}^{uRR} and δ_{23}^{dRR} . We see in 5(a) a constant QFC one-loop contribution of $\sim -10\%$ and $\sim 3\%$ variation due to QFV. The EW part can become up to $\sim 35\%$ of the SQCD one (5(b)) for large $|\delta_{23}^{uRR}|$ where the $\tilde{u}_1 t$ mode becomes important, since the \tilde{u}_1 mass becomes smaller due to the \tilde{u} -sector right-right mixing effect. Furthermore, as \tilde{u}_1 is mainly a top squark, the EW corrections to the $\tilde{u}_1 t$ mode are significant, mainly controlled by the large top-quark Yukawa coupling Y_t .

We also have studied the gluino mass dependence. The full one-loop corrections to the total width are of the order of about -10% in the gluino mass range of 2.3 - 4.0 TeV.

5. Conclusions

All gluino two-body decays at full one-loop level in the MSSM with QFV were studied. Numerically we have focused on a scenario where only the decays to $\tilde{u}_{1,2}$ and $\tilde{d}_{1,2}$ are kinematically open and \tilde{u}_1 is a mixture of \tilde{c}_R and \tilde{t}_R controlled by δ_{23}^{uRR} , and \tilde{d}_1 is a mixture of \tilde{s}_R and \tilde{b}_R controlled by δ_{23}^{dRR} . We obey the constraints from B-physics, the LHC constraints for the masses of the SUSY particles, especially that one for m_{h^0} and have checked also the vacuum stability conditions.

The full one-loop corrections to the gluino decay widths are mostly negative. For the total decay width they are in the range of -10% with a weak dependence on QFV parameters for both SQCD (gluon and gluino) and electroweak (includes also the photon) corrections. For the decay width into \tilde{u}_1 we can have a total correction up to -18% , with the electroweak part up to -8% , strongly depending on the QFV parameters, for \tilde{d}_1 the effects are smaller. In the branching ratios these effects are washed out. In general, it turns out that the EW corrections can be in the range of up to 35% of the SQCD corrections due to the large top-quark Yukawa coupling.

Acknowledgments

This work is supported by the "Fonds zur Förderung der wissenschaftlichen Forschung (FWF)" of Austria, project No. P26338-N27. We thank S. Frank for providing the program FVSFOLD.

References

- [1] W. Beenakker, R. Höpker and P. M. Zerwas, Phys. Lett. B **378** (1996) 159 [hep-ph/9602378].
- [2] S. Heinemeyer and C. Schappacher, Eur. Phys. J. C **72** (2012) 1905 [arXiv:1112.2830 [hep-ph]].
- [3] T. Hurth and W. Porod, JHEP **0908** (2009) 087 [arXiv:0904.4574 [hep-ph]].
- [4] A. Bartl, K. Hidaka, K. Hohenwarter-Sodek, T. Kernreiter, W. Majerotto and W. Porod, Phys. Lett. B **679** (2009) 260 [arXiv:0905.0132 [hep-ph]].
- [5] A. Bartl, H. Eberl, E. Ginina, B. Herrmann, K. Hidaka, W. Majerotto and W. Porod, Phys. Rev. D **84** (2011) 115026 [arXiv:1107.2775 [hep-ph]].
- [6] H. Eberl, E. Ginina, and K. Hidaka, Eur. Phys. J. C **77** (2017) no.3, 189 [arXiv:1702.00348 [hep-ph]].
- [7] S. Frank, "Quark flavour violating decays in supersymmetry", PhD thesis, available online at: <http://katalog.ub.tuwien.ac.at/AC11731597>
- [8] T. Hahn, Comput. Phys. Commun. **140** (2001) 418 [hep-ph/0012260],
- [9] T. Hahn, C. Schappacher, Comput. Phys. Commun. **143** (2002) 54 [hep-ph/0105349].
- [10] T. Hahn and M. Perez-Victoria, Comput. Phys. Commun. **118** (1999) 153 [hep-ph/9807565].
- [11] G.J. van Oldenborgh, Z. Phys. C **46** (1990) 425.
- [12] W. Porod, Comput. Phys. Commun. **153** (2003) 275 [hep-ph/0301101].
- [13] W. Porod and F. Staub, Comput. Phys. Commun. **183** (2012) 2458 [arXiv:1104.1573 [hep-ph]].